

Lattice QCD calculation of the two-photon exchange contribution to the muonic-hydrogen Lamb shift

Yang Fu^{a,*}

^a*School of Physics, Peking University, Beijing 100871, China*

E-mail: fy_deg@pku.edu.cn

We develop a method for lattice QCD calculation of the two-photon exchange (TPE) contribution to the muonic-hydrogen Lamb shift. To demonstrate the feasibility of this method, we also present an exploratory study with a gauge ensemble at $m_\pi = 142$ MeV. By adopting the infinite-volume reconstruction (IVR) method along with an optimized subtraction scheme, we obtain a preliminary result of the TPE contribution which agrees well with previous calculation using other methods and one magnitude smaller compare to the large ~ 300 μeV discrepancy for the proton radius puzzle.

*The 38th International Symposium on Lattice Field Theory, LATTICE2021 26th-30th July, 2021
Zoom/Gather@Massachusetts Institute of Technology*

*Speaker

1. Introduction

The measurement of muonic-hydrogen spectroscopy [1, 2] not only provides the most precise determination of the proton charge radius, but also raises the unexpected proton radius puzzle. This puzzle triggers a great deal of efforts to improve the theoretical corrections to both spectroscopy and scattering. Among them, the two-photon exchange (TPE) correction, see Fig. 1, is of special interest. It involves a wealth of information about the proton structure and introduces the largest theoretical uncertainty to both the Lamb shift and hyperfine splitting in muonic-hydrogen [3]. The TPE correction also plays an important role in the electron-proton scattering since it could be responsible for the drastic difference in the ratio of the proton electric to magnetic form factors obtained using the Rosenbluth separation [4] and the polarization transfer methods [5].

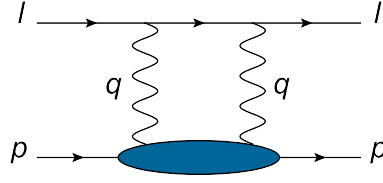


Figure 1: The diagram for two-photon exchange correction.

Several approaches have been applied in previous work, including dispersion relations (DR) [6–10], baryon χPT ($\text{B}\chi\text{PT}$) [11, 12], heavy baryon χPT ($\text{HB}\chi\text{PT}$) [13–15], non-relativistic QED (NRQED) [16] and operator product expansion (OPE) [17]. For these methods, the TPE correction is usually divided into Born and non-Born pieces, where as in the DR approach, the Born part can be well-constrained by the experiment data, but the non-Born part contains a component, commonly referred as "subtraction function", which is poorly constrained and relies on model, thus leading to a large systematic uncertainty. Other theoretical approaches are usually devoted to improve the determination of the non-Born contribution, in particular the contribution of subtraction function. It has also been recently proposed that the subtraction function can be further constrained by the dilepton electroproduction [18].

The total $2S - 2P$ Lamb shift in muonic hydrogen is given by [3] (units in meV and fm)

$$\Delta E_{\text{LS}}^{\text{theory}} = 206.0336(15) - 5.2275(10)\langle r_p^2 \rangle + \Delta E_{\text{TPE}}, \quad (1)$$

with their choice of TPE contribution $\Delta E_{\text{TPE}} = 0.0332(20)$ meV [8, 14] and experiment result $\Delta E_{\text{LS}}^{\text{exp}} = 202.3706(23)$ meV [2]. One find that the uncertainty of the TPE is at the same level as the present experimental precision, thus any further improvement on proton charge radius extraction from μH Lamb shift will unavoidably require an improved TPE determination, of which the precise lattice QCD calculation is undoubtedly important.

Several lattice QCD approaches have been recently proposed, including using the Feynman-Hellmann theorem to calculate the structure function [19] and using an unconventional choice of the subtraction point to calculate the non-Born contribution of the TPE [20]. In this work, we develop a method to directly calculate the TPE correction to the μH Lamb shift on the lattice. We also perform an exploratory study with a gauge ensemble at the physical pion mass. The preliminary result is consistent with previous data-driven analysis.

2. Two-photon exchange contribution

We start with the spin-averaged forward doubly-virtual Compton scattering (VVCS) tensor in Euclidean space. With $H_{\mu\nu}(x) = \langle p | \mathcal{T} [j_\mu(x) j_\nu(0)] | p \rangle$, we have

$$T_{\mu\nu}(P, Q) = \frac{1}{8\pi M} \int d^4x e^{iQ \cdot x} H_{\mu\nu}(x) \\ = \left(-\delta_{\mu\nu} + \frac{Q_\mu Q_\nu}{Q^2} \right) T_1(\nu, Q^2) - \left(P_\mu - \frac{P \cdot Q}{Q^2} Q_\mu \right) \left(P_\nu - \frac{P \cdot Q}{Q^2} Q_\nu \right) \frac{T_2(\nu, Q^2)}{M^2}, \quad (2)$$

where $\nu = P \cdot Q/M$ with P and Q the Euclidean proton and photon four-momenta, and M is the proton mass.

For the TPE contribution, the Euclidean momenta are chosen as $P = (iM, \vec{0})$ and $Q = (Q_0, \vec{Q})$. The relative energy shift to the the nS -state is then given by [6]

$$\Delta E = \frac{8m\alpha^2}{\pi} |\phi_n(0)|^2 \int d^4Q \frac{(Q^2 + 2Q_0^2)T_1(iQ_0, Q^2) - (Q^2 - Q_0^2)T_2(iQ_0, Q^2)}{Q^4(Q^4 + 4m^2Q_0^2)}. \quad (3)$$

where m is the lepton mass, $|\phi_n^2(0)| = m_r^3 \alpha^3 / (\pi n^3)$ is the square of the nS -state wave function at the origin with $m_r = mM/(M+m)$ the reduced mass. Note that the nP -state wave function vanishes at the origin, hence it won't receive any corrections from TPE at this order. Eq.(3) essentially contains an infrared singularity which is due to the terms already accounted for at the lower order [8]: one is the point-like proton contribution, which means the proton-photon vertex function $\Gamma_\mu = \gamma_\mu$, hence

$$T_1^{(\text{pt})} = \frac{M}{\pi} \frac{\nu^2}{Q^4 - 4M^2\nu^2}, \quad T_2^{(\text{pt})} = \frac{M}{\pi} \frac{Q^2}{Q^4 - 4M^2\nu^2}, \quad (4)$$

another one is the charge radius term from third Zemach moment contribution

$$\Delta E^{(\text{Z})} = -\alpha^2 |\phi_n(0)|^2 \int \frac{dQ^2}{Q^2} \frac{16mM}{(M+m)Q} G'_E(0), \quad (5)$$

with $G_E(Q^2)$ the proton electric form factor and its derivative can be related to proton charge radius via $\langle r_p^2 \rangle = -6G'_E(0)$. These terms should be subtracted in order to both keep the TPE contribution IR finite and avoid double-counting.

3. Lattice QCD methodology

On the lattice, we prefer to rewrite Eq.(3) in terms of T_{00} and $\sum_i T_{ii}$

$$\Delta E = -16m\alpha^2 |\phi_n(0)|^2 \int \frac{dQ^2}{Q^2} \int_{-\frac{\pi}{2}}^{\frac{\pi}{2}} d\theta \left(g_1 T_{00} + g_2 \sum_i T_{ii} \right), \quad (6)$$

with

$$g_1 = \frac{1 - \sin^4 \theta}{Q^2 + 4m^2 \sin^2 \theta}, \quad g_2 = \frac{\sin^2 \theta (1 - \sin^2 \theta)}{Q^2 + 4m^2 \sin^2 \theta}, \quad (7)$$

and the angle θ defined as

$$Q_0 = Q \sin \theta, \quad |\vec{Q}| = Q \cos \theta. \quad (8)$$

The point-like proton contribution from Eq.(4) can also be represented in terms of T_{00} and $\sum_i T_{ii}$

$$T_{00}^{(\text{pt})} = \frac{M}{\pi} \frac{Q^2 - Q_0^2}{Q^4 + 4M^2 Q_0^2}, \quad \sum_i T_{ii}^{(\text{pt})} = \frac{M}{\pi} \frac{3Q_0^2}{Q^4 + 4M^2 Q_0^2}. \quad (9)$$

Combining Eq.(2) and (6), we obtain

$$\Delta E = \frac{2m\alpha^2}{\pi M} |\phi_n(0)|^2 \sum_{i=1,2} \int d^4x \omega_i(\vec{x}, t) H_i(\vec{x}, t), \quad (10)$$

here the hadronic functions are defined as $H_1(\vec{x}, t) = H_{00}(\vec{x}, t)$ and $H_2(\vec{x}, t) = \sum_i H_{ii}(\vec{x}, t)$, with weight functions given by

$$\omega_i(\vec{x}, t) = - \int \frac{dQ^2}{Q^2} \int_{-\pi/2}^{\pi/2} d\theta f(Q; x) g_i, \quad f(Q; x) = \cos(Q_0 t) j_0(|\vec{Q}| |\vec{x}|), \quad (11)$$

where an average over the spatial directions is taken and $j_n(x)$ are the spherical Bessel functions. One immediately find these weight functions are IR divergent since we have not performed the subtraction.

The IR divergence occurs only in the elastic contribution, then both of the two terms given by Eq.(5) and (9) can be reproduced by the ground-state contribution on the lattice. Choosing a sufficiently large time t_s for the ground-state saturation, we obtain that

$$\begin{aligned} \tilde{H}_i(\vec{Q}, t_s) &= \int d^3\vec{x} j_0(|\vec{Q}| |\vec{x}|) H_i(\vec{x}, t_s) \\ &= \frac{M}{E_Q} e^{-(E_Q - M)t_s} \times \begin{cases} (E_Q + M) G_E^2(Q_{\text{on}}^2), & i = 1, \\ -(E_Q - M) [G_E^2 + 2G_M^2](Q_{\text{on}}^2), & i = 2, \end{cases} \end{aligned} \quad (12)$$

here G_E, G_M are the proton electric and magnetic form factors, with $E_Q = \sqrt{M^2 + \vec{Q}^2}$ the proton energy and $Q_{\text{on}}^2 = 2M(E_Q - M)$. The low-momentum expansion of Eq.(12) gives that

$$G_E^2(0) = \int d^3\vec{x} L_0(\vec{x}, t_s) H_1(\vec{x}, t_s), \quad \langle r_p^2 \rangle = \int d^3\vec{x} L_r(\vec{x}, t_s) H_1(\vec{x}, t_s), \quad (13)$$

with

$$L_0(\vec{x}, t_s) = \frac{1}{2M}, \quad L_r(\vec{x}, t_s) = \frac{1}{4M} \left(x^2 - \frac{3 + 6Mt_s}{2M^2} \right). \quad (14)$$

The similar idea has been applied to the pion electromagnetic transition to extract the charge radius [21]. The terms need to be subtracted can then be given by

$$\Delta E^{(\text{sub})} = \frac{2m\alpha^2}{\pi M} |\phi_n(0)|^2 \int d^3\vec{x} L^{(\text{sub})}(\vec{x}, t_s) H_1(\vec{x}, t_s),$$

with three different weight functions $L^{(\text{sub})}(\vec{x}, t_s)$

$$\begin{aligned} L_{00}^{(\text{pt})}(\vec{x}, t_s) &= - \int \frac{dQ^2}{Q^2} \int_{-\pi/2}^{\pi/2} d\theta S_1(Q) g_1, \\ L_{ii}^{(\text{pt})}(\vec{x}, t_s) &= - \int \frac{dQ^2}{Q^2} \int_{-\pi/2}^{\pi/2} d\theta S_2(Q) g_2, \\ L^{(Z)}(\vec{x}, t_s) &= \int \frac{dQ^2}{Q^2} \frac{4\pi M^2}{3(M+m)Q} L_r(\vec{x}, t_s). \end{aligned} \quad (15)$$

here

$$S_1(Q) = 8\pi M T_{00}^{(\text{pt})} L_0(\vec{x}, t_s) = \frac{4M(Q^2 - Q_0^2)}{Q^4 + 4M^2 Q_0^2}, \quad S_2(Q) = 8\pi M \sum_i T_{ii}^{(\text{pt})} L_0(\vec{x}, t_s) = \frac{12M Q_0^2}{Q^4 + 4M^2 Q_0^2}. \quad (16)$$

The subtraction of the hadronic matrix elements has therefore been transferred to the subtraction of weight functions, which facilitates the lattice QCD calculation.

We further adopt the infinite-volume reconstruction (IVR) method [22], which is developed to remove all the power-law finite-volume effects in the QED self-energy [23]. This method has been successfully applied to the lattice study of double beta decays [24], rare decays [25] and the leptonic decays [26, 27]. In the work, the IVR method plays a crucial role in the removal of the infrared divergence. In practise, the time integral in Eq.(2) is split into the range of $|t| < t_s$ and $|t| > t_s$

$$T_{\mu\nu} = \frac{1}{8\pi M} \left[\int_{|t| < t_s} d^4x f(Q; x) H_{\mu\nu}(\vec{x}, t) + \int d^3\vec{x} S(Q; \vec{x}, t_s) H_{\mu\nu}(\vec{x}, t_s) \right], \quad (17)$$

with

$$\begin{aligned} S(Q; \vec{x}, t_s) &= 2 \int \frac{d^3\vec{Q}}{(2\pi)^3} e^{i\vec{Q}\cdot\vec{x}} \int_{t_s}^{\infty} dt e^{-(E_Q - M)(t - t_s)} \int d^3\vec{x}' e^{-i\vec{Q}\cdot\vec{x}'} f(Q; x) \\ &= \frac{4MQ^2}{Q^4 + 4M^2 Q_0^2} A(Q; t_s) j_0(|\vec{Q}||\vec{x}|), \end{aligned} \quad (18)$$

here

$$A(Q; t_s) = A_c(Q) \cos(Q_0 t_s) - A_s(Q) \sin(Q_0 t_s), \quad (19)$$

and the auxiliary functions are

$$A_c(Q) = \sqrt{\frac{1}{4} + \tau_p \cos^2 \theta + \frac{1}{2} - \sin^2 \theta}, \quad A_s(Q) = \frac{\sin \theta}{\sqrt{\tau_p}} \left(\sqrt{\frac{1}{4} + \tau_p \cos^2 \theta + \frac{1}{2} + \tau_p} \right). \quad (20)$$

with $\tau_p = Q^2/(4M^2)$ and the angle θ defined in Eq.(8). Correspondingly, the time integral in ΔE can be also split into

$$\begin{aligned} \Delta E_{|t| < t_s} &= \frac{2m\alpha^2}{\pi M} |\phi_n(0)|^2 \sum_{i=1,2} \int_{|t| < t_s} d^4x \omega_i(\vec{x}, t) H_i(\vec{x}, t), \\ \Delta E_{|t| > t_s} &= \frac{2m\alpha^2}{\pi M} |\phi_n(0)|^2 \sum_{i=1,2} \int d^3\vec{x} L_i(\vec{x}, t_s) H_i(\vec{x}, t_s), \end{aligned} \quad (21)$$

here the weight functions $L_i(\vec{x}, t_s)$ are given by

$$L_i(\vec{x}, t_s) = - \int \frac{dQ^2}{Q^2} \int_{-\frac{\pi}{2}}^{\frac{\pi}{2}} d\theta S(Q; \vec{x}, t_s) g_i. \quad (22)$$

Currently both two types of weight functions $\omega_i(\vec{x}, t)$ and $L_i(\vec{x}, t_s)$ are IR divergent, but the subtraction is only performed to the latter. Considering that the ΔE should be finite, these weight functions will still be IR divergent even after performing the subtraction. The hadronic functions

from $|t| < t_s$ and $|t| > t_s$, however, can be constrained by the low-energy expansion (LEX) of the VVCS tensor, thus are not completely unrelated. The LEX of $T_{\mu\nu}$ gives [28]

$$T_{\mu\nu}(Q) = T_{\mu\nu}^{\text{Born}}(Q) + \mathcal{O}(Q^2), \quad (23)$$

where the Born terms are standard [8, 14, 28]. Comparing this LEX with Eq.(12) and (17) in the low- Q limit, we find that

$$\frac{1}{8\pi M} \int_{|t| < t_s} d^4x [H_i(\vec{x}, t) - H_i(\vec{x}, t_s)] = \begin{cases} 0, & i = 1, \\ \frac{3}{4\pi M}, & i = 2. \end{cases} \quad (24)$$

This relation ensures that the IR divergence of $\omega_i(\vec{x}, t)$ and $L_i(\vec{x}, t_s)$ can be exactly canceled out. We modify these weight functions to

$$\omega_i(\vec{x}, t) = - \int \frac{dQ^2}{Q^2} \int_{-\frac{\pi}{2}}^{\frac{\pi}{2}} d\theta [f(Q; x) - 1] g_i, \quad (25)$$

and

$$L_i(\vec{x}, t_s) = - \int \frac{dQ^2}{Q^2} \int_{-\frac{\pi}{2}}^{\frac{\pi}{2}} d\theta [S(Q; \vec{x}, t_s) + 2t_s] g_i, \quad (26)$$

which does not change the contribution from temporal component T_{00} , but does remove a term of $3/(4\pi M)$ from the spatial component $\sum_i T_{ii}$ hence needs to be added back. Such term can be directly combined with the subtraction of $\sum_i T_{ii}^{(\text{pt})}$ defined in Eq.(9) and leaves a term of $\frac{3}{4\pi M} \left(\frac{Q^4}{Q^4 - 4M^2 v^2} \right)$ which contributes a finite $-0.60 \mu\text{eV}$ to the total TPE energy shift. Finally, after performing the subtraction of remaining contribution from $L_{00}^{(\text{pt})}(\vec{x}, t_s)$ and $L^{(Z)}(\vec{x}, t_s)$, we obtain that

$$L_i(\vec{x}, t_s) = - \int \frac{dQ^2}{Q^2} \left\{ \int_{-\frac{\pi}{2}}^{\frac{\pi}{2}} d\theta \left([S - S_1](Q; \vec{x}, t_s) + 2t_s \right) g_i + \frac{4\pi M^2}{3(M+m)Q} L_r(\vec{x}, t_s) \delta_{i,1} \right\}, \quad (27)$$

with $S_1(Q; \vec{x}, t_s) = S_1(Q)$. Here a trivial subtraction is also applied to $L_2(\vec{x}, t_s)$ to make it IR finite, since Eq.(12) shows that $\int d^3\vec{x} H_2(\vec{x}, t_s) = 0$.

4. Optimized subtraction scheme

Eq.(21) along with the weight functions given by Eq.(25) and (27) provides a direct way to calculate the TPE contribution using hadronic functions $H_i(\vec{x}, t)$ as input, but it suffers from both the finite-volume effects and the signal-to-noise problem in a realistic lattice QCD calculation, due to the fact that $L_1(\vec{x}, t_s)$ increases rapidly as the spatial distance $|\vec{x}|$ increases. However, not all the contributions from $L_1(\vec{x}, t_s)$ need to be determined on the lattice. Inspired by Eq.(1), We can divide the ΔE into

$$\Delta E = -0.60 \mu\text{eV} + c_0 + c_r \langle r_p^2 \rangle + \Delta E^{(\text{lat})}, \quad (28)$$

by splitting the weight function $L_1(\vec{x}, t_s)$

$$L_1(\vec{x}, t_s) = \bar{c}_0 L_0(\vec{x}, t_s) + \bar{c}_r L_r(\vec{x}, t_s) + L_1^{(r)}(\vec{x}, t_s), \quad (29)$$

with $\bar{c} = c / \left(\frac{2m\alpha^2}{\pi M} |\phi_n(0)|^2 \right)$. As a result, only the $\Delta E^{(\text{lat})}$ need to be calculated on the lattice using the reduced weight function $L_1^{(r)}(\vec{x}, t_s)$ along with other three weight functions. The choice of two coefficients c_0 and c_r can be viewed as a subtraction scheme. We choose them by minimizing the following integral

$$\int_{R_{\min}}^{R_{\max}} dx 4\pi x^2 [L_1(x, t_s) - \bar{c}_0 L_0(x, t_s) - \bar{c}_r L_r(x, t_s)]^2. \quad (30)$$

with sufficiently large t_s for ground state saturation, as well as the range R_{\min} to R_{\max} dominants the contribution of the integral. In this way, the long-distance contribution can be almost completely represented by the charge conservation and charge radius terms, which eliminates the need for lattice data as input.

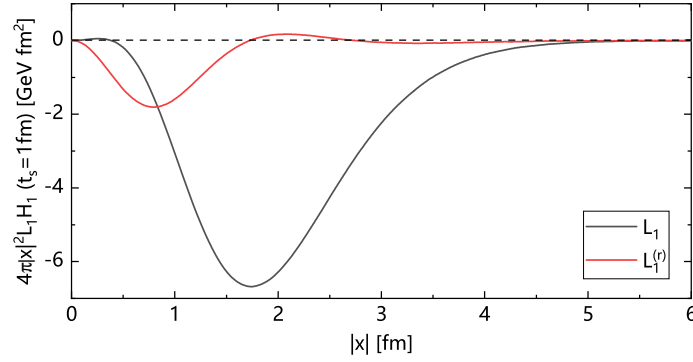


Figure 2: The integrand $4\pi|\vec{x}|^2 L_1(\vec{x}, t_s) H_1(\vec{x}, t_s)$ as a function of $|\vec{x}|$ estimated by the dipole form factor.

We set $t_s = 1$ fm for the ground-state saturation, as a result the hadronic function $H_1(\vec{x}, t_s)$ can be estimated by the proton form factor. By using a dipole functional form $G_E(Q^2) = 1/(1 + Q^2\langle r_p^2 \rangle/12)^2$ with $\sqrt{\langle r_p^2 \rangle} = 0.85$ fm for the form factor, the result of the integrand $4\pi|\vec{x}|^2 L_1(\vec{x}, t_s) H_1(\vec{x}, t_s)$ as a function of $|\vec{x}|$ is shown in Fig. 2. We find that the contribution of this integral mainly comes from the range of 1 – 3 fm, while the saturation occurs at around 5 fm, which requires a large spatial volume $L \simeq 10$ fm. We thus set R_{\min} and R_{\max} as 1 fm and 3 fm. With these parameters, the coefficients can be obtained as $c_0 = -0.17 \mu\text{eV}$ and $c_r = -93.72 \mu\text{eV}/\text{fm}^2$. As shown in Fig. 2, we now find the saturation for $L_1^{(r)}(\vec{x}, t_s)$ term occurs at around 2.5 fm, which means the long-distance contribution is significantly reduced compared to the original $L_1(\vec{x}, t_s)$ term. Finally, the TPE correction to the $2S - 2P$ μH Lamb shift is given by

$$\Delta E_{\text{TPE}} = 0.77 \mu\text{eV} + 93.72 \mu\text{eV}/\text{fm}^2 \langle r_p^2 \rangle - \Delta E^{(\text{lat})}. \quad (31)$$

Here a minus sign is added due to the TPE correction is only applied to the nS -state.

5. Numerical result

In this exploratory study, we have used a single gauge ensemble at physical point $m_\pi = 142$ MeV, generated by the RBC and UKQCD Collaborations using 2 + 1-flavor domain wall fermion

[29]. The corresponding parameters are listed in Table 1. We calculate the four-point correlation function $\sum_{\vec{x}_f, \vec{x}_i} \mathcal{P} \langle \psi_p(\vec{x}_f, t_f) j_\mu(x) j_\nu(y) \psi_p^\dagger(\vec{x}_i, t_i) \rangle$ using the field sparsening technique [30, 31], with the projection matrix $\mathcal{P} = (1 + \gamma_0)/2$ and the time slices chosen as $t_i = \min\{t_x, t_y\} - \Delta t$, $t_f = \max\{t_x, t_y\} + \Delta t$. The Δt should be sufficiently large for the proton ground-state saturation, but as the Δt increases, the signal-to-noise problem will also be dramatically enhanced. In this exploratory study, Δt is chosen to be $2a = 0.39$ fm. There are five types of contractions for the TPE diagrams as shown in Fig. 3. The first two are quark connected diagrams, while the last three are quark disconnected diagrams. Type IV and Type V are neglected in this work since they vanish in the flavor SU(3) limit. We use the gauge configurations with sufficiently long separation, i.e., each separated by at least 10 trajectories.

Ensemble	m_π [MeV]	L	T	a [fm]	N_{conf}	$\Delta t/a$
24D	142	24	64	0.1944	131	2

Table 1: Ensemble used in this work. We list the pion mass m_π , the spatial and temporal extents, L and T , the lattice spacing a , the number of configurations used N_{conf} , and the time-separation Δt used for the ground-state saturation.

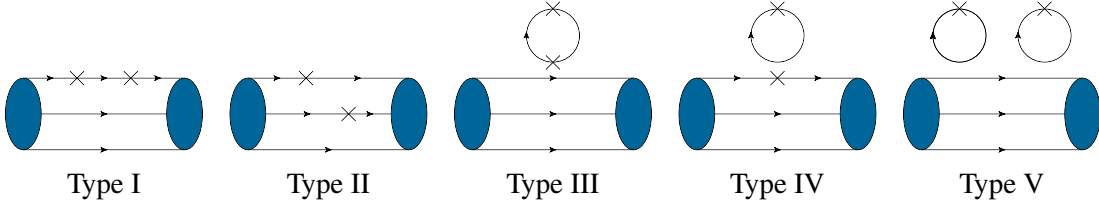


Figure 3: Five types of quark contractions for TPE diagrams. The blob denotes a proton state. Type I: two currents on the same quark line. Type II: two currents on different quark lines. Type III, IV, V: quark disconnected diagrams. The last two types are neglected in this work.

In practice, the integral in Eq.(21) can be performed within a range of $|\vec{x}| < R$ for any choice of time t_s . Here we take $t_s = 4a = 0.79$ fm as an example. As shown in the left panel of Fig. 4, all four terms in the integral is saturated at large R for both connected and disconnected contributions. This indicates the finite-volume effects are well under control in our calculation.

The results of $\Delta E^{(\text{lat})}$ as a function of t_s are shown in the right panel of Fig. 4. We find a plateau starting from $t_s = 4a = 0.79$ fm. The results are in good agreement with results from data-driven analysis and one magnitude smaller compared to the large ~ 300 μeV discrepancy for the proton radius puzzle.

The systematic error of our result should mainly come from the excited-states contamination and the lattice discretization error, which requires results from multiple choices of Δt and lattice spacing a . Further calculations and analyses are in progress.

6. Conclusion

We have developed a method to calculate the two-photon exchange correction to the muonic-hydrogen Lamb shift using lattice QCD. We also find that the long-distance contribution can

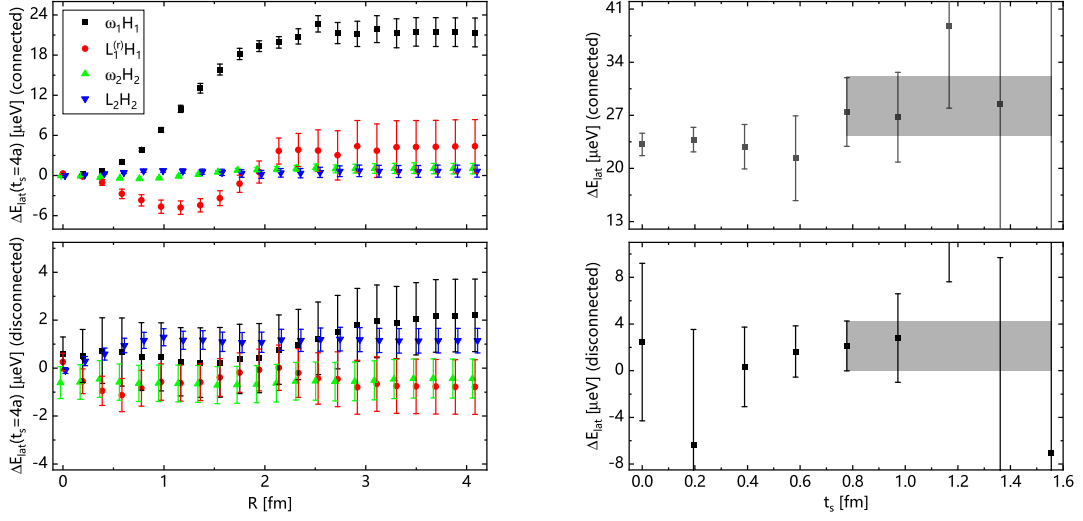


Figure 4: Left: $\Delta E^{(\text{lat})}$ as a function of the integral range R at $t_s = 4a$. Results from different terms have been slightly shifted for clarity. Right: $\Delta E^{(\text{lat})}$ as a function of t_s . For both left and right figure, the upper and lower panels show the results for the connected and disconnected contribution, respectively.

be reduced by adopting an optimized subtraction scheme, hence both the finite-volume effects and nucleon signal-to-noise problem are suppressed. A preliminary result at $m_\pi = 142$ MeV is presented here and it demonstrates the feasibility of our method.

This method can also be extended to other higher-order corrections, including the TPE corrections to other processes such as hyperfine splitting and electron-proton scattering. In a foreseeable future, lattice QCD should be able to give very precise calculations for these quantities, which is crucial for a better understanding and precise measurement of the nucleon internal structure.

References

- [1] R. Pohl et al., *The size of the proton*, *Nature* **466** (2010) 213.
- [2] A. Antognini et al., *Proton Structure from the Measurement of $2S - 2P$ Transition Frequencies of Muonic Hydrogen*, *Science* **339** (2013) 417.
- [3] A. Antognini, F. Kottmann, F. Biraben, P. Indelicato, F. Nez and R. Pohl, *Theory of the $2S-2P$ Lamb shift and $2S$ hyperfine splitting in muonic hydrogen*, *Annals Phys.* **331** (2013) 127 [1208.2637].
- [4] M.N. Rosenbluth, *High Energy Elastic Scattering of Electrons on Protons*, *Phys. Rev.* **79** (1950) 615.
- [5] JEFFERSON LAB HALL A collaboration, *$G(E(p)) / G(M(p))$ ratio by polarization transfer in polarized $e p \rightarrow e$ polarized p* , *Phys. Rev. Lett.* **84** (2000) 1398 [nuc1-ex/9910005].
- [6] K. Pachucki, *Proton structure effects in muonic hydrogen*, *Phys. Rev. A* **60** (1999) 3593 [physics/9906002].

- [7] A.P. Martynenko, *Proton polarizability effect in the Lamb shift of the hydrogen atom*, *Phys. Atom. Nucl.* **69** (2006) 1309 [[hep-ph/0509236](#)].
- [8] C.E. Carlson and M. Vanderhaeghen, *Higher order proton structure corrections to the Lamb shift in muonic hydrogen*, *Phys. Rev. A* **84** (2011) 020102 [[1101.5965](#)].
- [9] M. Gorchtein, F.J. Llanes-Estrada and A.P. Szczepaniak, *Muonic-hydrogen Lamb shift: Dispersing the nucleon-excitation uncertainty with a finite-energy sum rule*, *Phys. Rev. A* **87** (2013) 052501 [[1302.2807](#)].
- [10] O. Tomalak, *Two-Photon Exchange Correction to the Lamb Shift and Hyperfine Splitting of S Levels*, *Eur. Phys. J. A* **55** (2019) 64 [[1808.09204](#)].
- [11] J.M. Alarcon, V. Lensky and V. Pascalutsa, *Chiral perturbation theory of muonic hydrogen Lamb shift: polarizability contribution*, *Eur. Phys. J. C* **74** (2014) 2852 [[1312.1219](#)].
- [12] J.M. Alarcón, F. Hagelstein, V. Lensky and V. Pascalutsa, *Forward doubly-virtual Compton scattering off the nucleon in chiral perturbation theory: the subtraction function and moments of unpolarized structure functions*, *Phys. Rev. D* **102** (2020) 014006 [[2005.09518](#)].
- [13] D. Nevado and A. Pineda, *Forward virtual Compton scattering and the Lamb shift in chiral perturbation theory*, *Phys. Rev. C* **77** (2008) 035202 [[0712.1294](#)].
- [14] M.C. Birse and J.A. McGovern, *Proton polarisability contribution to the Lamb shift in muonic hydrogen at fourth order in chiral perturbation theory*, *Eur. Phys. J. A* **48** (2012) 120 [[1206.3030](#)].
- [15] C. Peset and A. Pineda, *The Lamb shift in muonic hydrogen and the proton radius from effective field theories*, *Eur. Phys. J. A* **51** (2015) 156 [[1508.01948](#)].
- [16] R.J. Hill and G. Paz, *Model independent analysis of proton structure for hydrogenic bound states*, *Phys. Rev. Lett.* **107** (2011) 160402 [[1103.4617](#)].
- [17] R.J. Hill and G. Paz, *Nucleon spin-averaged forward virtual Compton tensor at large Q^2* , *Phys. Rev. D* **95** (2017) 094017 [[1611.09917](#)].
- [18] V. Pauk, C.E. Carlson and M. Vanderhaeghen, *Low-energy doubly virtual Compton scattering from dilepton electroproduction on a nucleon*, *Phys. Rev. C* **102** (2020) 035201 [[2001.10626](#)].
- [19] K.U. Can et al., *Lattice QCD evaluation of the Compton amplitude employing the Feynman-Hellmann theorem*, *Phys. Rev. D* **102** (2020) 114505 [[2007.01523](#)].
- [20] F. Hagelstein and V. Pascalutsa, *The subtraction contribution to muonic-hydrogen Lamb shift: a point for lattice QCD calculation of polarizability effect*, [2010.11898](#).
- [21] X. Feng, Y. Fu and L.-C. Jin, *Lattice QCD calculation of the pion charge radius using a model-independent method*, *Phys. Rev. D* **101** (2020) 051502 [[1911.04064](#)].

- [22] X. Feng and L. Jin, *QED self energies from lattice QCD without power-law finite-volume errors*, *Phys. Rev. D* **100** (2019) 094509 [1812.09817].
- [23] X. Feng, L. Jin and M.J. Riberdy, *Lattice QCD calculation of the pion mass splitting*, 2108.05311.
- [24] X.-Y. Tuo, X. Feng and L.-C. Jin, *Long-distance contributions to neutrinoless double beta decay $\pi^- \rightarrow \pi^+ ee$* , *Phys. Rev. D* **100** (2019) 094511 [1909.13525].
- [25] N.H. Christ, X. Feng, L.-C. Jin and C.T. Sachrajda, *Finite-volume effects in long-distance processes with massless leptonic propagators*, *Phys. Rev. D* **103** (2021) 014507 [2009.08287].
- [26] N.H. Christ, X. Feng, J. Lu-Chang and C.T. Sachrajda, *Electromagnetic corrections to leptonic pion decay from lattice QCD using infinite-volume reconstruction method*, *PoS LATTICE2019* (2020) 259.
- [27] X.-Y. Tuo, X. Feng, L.-C. Jin and T. Wang, *Lattice QCD calculation of $K \rightarrow \ell \nu_\ell \ell'^+ \ell'^-$ decay width*, 2103.11331.
- [28] J. Gasser, M. Hoferichter, H. Leutwyler and A. Rusetsky, *Cottingham formula and nucleon polarisabilities*, *Eur. Phys. J. C* **75** (2015) 375 [1506.06747].
- [29] RBC, UKQCD collaboration, *Domain wall QCD with physical quark masses*, *Phys. Rev. D* **93** (2016) 074505 [1411.7017].
- [30] W. Detmold, D.J. Murphy, A.V. Pochinsky, M.J. Savage, P.E. Shanahan and M.L. Wagman, *Sparsening algorithm for multihadron lattice QCD correlation functions*, *Phys. Rev. D* **104** (2021) 034502 [1908.07050].
- [31] Y. Li, S.-C. Xia, X. Feng, L.-C. Jin and C. Liu, *Field sparsening for the construction of the correlation functions in lattice QCD*, *Phys. Rev. D* **103** (2021) 014514 [2009.01029].